Development of the camera for the Large Size Telescopes of the Cherenkov Telescope Array

Y. Inome[1], G. Ambrosi[2], Y. Awane[3], H. Baba[4], A. Bamba[5], M. Barceló[6], U. Barres de Almeida[7], J.A. Barrio[8], O. Blanch Bigas[6], J. Boix[6], L. Brunetti[9], E. Carmona[10], E. Chabanne[9], M. Chikawa[11], N. Cho[4], P. Colin[12], J.L. Conteras[8], J. Cortina[6], F. Dazzi[13], A. Deangelis[14], G. Deleglise[9], C. Delgado[10], C. Díaz[10], F. Dubois[8], A. Fiasson[9], D. Fink[12], N. Fouque[9], L. Freixas[10], C. Fruck[12], A. Gadola[15], R. García[16], D. Gascón[17], N. Geffroy[9], N. Giglietto[18], F. Giordano[18], F. Grañena[6], S. Gunji[19], R. Hagiwara[19], N. Hamer[10], Y. Hanabata[20], T. Hassan[8], K. Hatanaka[3], T. Haubold[12], M. Hayashida[20], R. Hermel[9], D. Herranz[8], K. Hirotani[20], J. Hose[12], D. Hugh[12], S. Inoue[20], Y. Inoue[20], K. Ioka[21], C. Jablonski[12], M. Kagaya[4], H. Katagiri[4], J. Kataoka[22], H. Kellermann[12], T. Kishimoto[3], M. Knoetig[12], K. Kodani[23], K. Kohri[21], T. Kojima[20], Y. Konno[3], S. Koyama[24], H. Kubo[3], J. Kushida[23], G. Lamanna[9], T. Le Flour[9], M. López-Moya[8], R. López[6], E. Lorenz[12], P. Majumdar[25], A. Manalaysay[15], M. Mariotti[13], G. Martínez[10], M. Martínez[6], S. Masuda[3], S. Matsuoka[26], D. Mazin[12], U. Menzel[12], J.M. Miranda[27], R. Mirzoyan[12], I. Monteiro[9], A. Moralejo[6], K. Murase[20], S. Nagataki[26], T. Nagayoshi[26], D. Nakajima[12,20], T. Nakamori[22], K. Nishijima[23], K. Noda[12], A. Nozato[11], M. Ogino[20], Y. Ohira[21], M. Ohishi[20], H. Ohoka[20], A. Okumura[28], S. Ono[4], R. Orito[29], J.L. Panazol[9], D. Paneque[12], R. Paoletti[30], J.M. Paredes[17], G. Pauletta[14], S. Podkladkin[12], J. Prast[9], R. Rando[13], O. Reimann[12], M. Ribó[17], S. Rosier-Lees[9], K. Saito[20], T. Saito[3], Y. Saito[23], N. Sakaki[20], R. Sakonaka[11], A. Sanuy[17], M. Sawada[5], V. Scalzotto[13], S. Schultz[13], T. Schweizer[12], T. Shibata[5], S. Shu[11], J. Sieiro[17], V. Stamatescu[6], S. Steiner[15], U. Straumann[15], R. Sugawara[29], H. Tajima[28], H. Takami[22], M. Takahashi[30], S. Tanaka[4], M. Tanaka[22], L.A. Tejedor[8], Y. Terada[24], M. Teshima[12,20], Y. Tomono[23], T. Totani[31], T, Toyama[12], Y. Tsubone[5], Y. Tsuchiya[3], S. Tsujimoto[23], H. Ueno[24], K. Umehara[4], Y. Umetsu[23], A. Vollhardt[15], R. Wagner[12], H. Wetteskind[12], T. Yamamoto[1], R. Yamazaki[5], A. Yoshida[5], T. Yoshida[4], T. Yoshikoshi[20], for The Cherenkov Telescope Array Consortium*

[1] Department of Physics, Konan University, Kobe, Hyogo, 658-8501 Japan;
[2] INFN Sezione di Perugia, Via A. Pascoli, Perugia, Italy;
[3] Kyoto University, Sakyo-ku, Kyoto 606-8502, Japan;
[4] Faculty of Science, Ibaraki University, Mito, Ibaraki, 310-8512, Japan;
[5] Department of Physics and Mathematics, Aoyama Gakuin University, Fuchinobe, Sagamihara, Kanagawa, 229-8558, Japan;
[6] Institut de Fsica d'Altes Energies (IFAE), Edifici Cn, Campus UAB, 08193 Bellaterra, Spain;
[7] Centro Brasileiro de Pesquisas Fisicas (CBPF/MCTI), Rua Xavier Sigaud 150, RJ 22290-180, Rio de Janeiro, Brazil;
[8] Grupo de Altas Energas, Universidad Complutense de Madrid, Av Complutense s/n, 28040 Madrid, Spain;
[9] LAPP, Universit ´ e de Savoie, CNRS/IN2P3, 9 Chemin de Bellevue - BP 110, 74941 Annecy-le-Vieux Cedex, France;
[10] CIEMAT, Avda. Complutense 22, 28040 Madrid, Spain;
[11] Department of Physics, Kinki University, Kowakae, Higashi-Osaka 577-8502, Japan;
[12] Max-Planck-Institut für Physik, Föhringer Ring 6, 80805 Mnchen, Germany;

Advances in Optical and Mechanical Technologies for Telescopes and Instrumentation, edited by Ramón Navarro, Colin R. Cunningham, Allison A. Barto, Proc. of SPIE Vol. 9151, 915142
 doi: 10.1117/12.2054619

[13] Dipartimento di Fisica - Universitá degli Studi di Padova, Via Marzolo 8, 35131 Padova, Italy;
[14] University of Udine & INFN Sezione di Trieste, Via delle Scienze 208, 33100 Udine, Italy;
[15] Physik-Institut, Universitt Zürich, Winterthurerstrasse 190, 8057 Zrich, Switzerland;
[16] Instituto de Astrofsica de Canarias (IAC), Via Lactea, 38205 La Laguna, Tenerife, Spain;
[17] Departament d'Astronomia i Meteorologia (ICC-UB), Universitat de Barcelona, Mart i Franqus, 1, 08028, Barcelona, Spain;
[18] INFN Sezione di Bari, via Orabona 4, I-70126 Bari, Italy;
[19] Department of Physics, Yamagata University, Yamagata, Yamagata 990-8560, Japan.
[20] Institute for Cosmic Ray Research (ICRR), University of Tokyo, 5-1-5, Kashi-wanoha, Kashiwa, Chiba 277-8582, Japan;
[21] Institute of Particle and Nuclear Studies, KEK, 1-1 Oho, Tsukuba, 305-0801, Japan;
[22] Faculty of Science and Engineering, Waseda University, Shinjuku, Tokyo 169-8555, Japan;
[23] Department of Physics, Tokai University, 1117 Kita-Kaname, Hiratsuka, Kanagawa 259-1292, Japan;
[24] Saitama University, 255 Simo-Ohkubo, Sakura-ku, Saitama city, Saitama 338-8570, Japan;
[25] Saha Institute of Nuclear Physics (SINP), Kolkata, India;
[26] RIKEN, Advanced Science Institute, 2-1 Hirosawa, Wako, Saitama 351-0198, Japan;
[27] Grupo de Electrnica, Universidad Complutense de Madrid, Av. Complutense s/n, 28040 Madrid, Spain;
[28] Nagoya University, Chikusa-ku, Nagoya 464-8602, Japan;
[29] Institute of Socio-Arts and Sciences, University of Tokushima, Tokushima 770-8502, Japan;
[30] Universit'a di Siena & INFN Sezione di Pisa, Via Roma 56, 53100 Siena, Italy;
[31] Department of Physics, Graduate School of Science, University of Tokyo, 7-3-1 Hongo, Bunkyo-ku, Tokyo 113-0033, Japan;

ABSTRACT

The Large Size Telescopes, LSTs, located at the center of the Cherenkov Telescope Array, CTA, will be sensitive for low energy gamma-rays. The camera on the LST focal plane is optimized to detect low energy events based on a high photon detection efficiency and high speed electronics. Also the trigger system is designed to detect low energy showers as much as possible. In addition, the camera is required to work stably without maintenance in a few tens of years. In this contribution we present the design of the camera for the first LST and the status of its development and production.

Keywords: Imaging Atmospheric Cherenkov Telescope, CTA, gamma-rays

1. INTRODUCTION

The Cherenkov Telescope Array (CTA) project aims to implement world痴 largest next generation of Very High Energy gamma-ray Imaging Atmospheric Cherenkov Telescopes devoted to the observation from a few tens of GeV to more than 100 TeV.[1] To view the whole sky, two CTA sites are foreseen, one for each hemisphere. The sensitivity at the lowest energy range will be dominated by four Large Size Telescopes (LSTs) located at the center of the array. Each LST has a parabolic mirror of 23 m diameter. The telescope is able to point all direction in the sky in 30 seconds to observe transit objects such as Gamma-Ray Bursts. The camera is mounted

Further author information: (Send correspondence to Y. Inome and T. Yamamoto)
Y. Inome: E-mail: m1321001@center.konan-u.ac.jp
T. Yamamoto: E-mail: tokonatu@konan-u.ac.jp
∗ http://cta-observatory.org

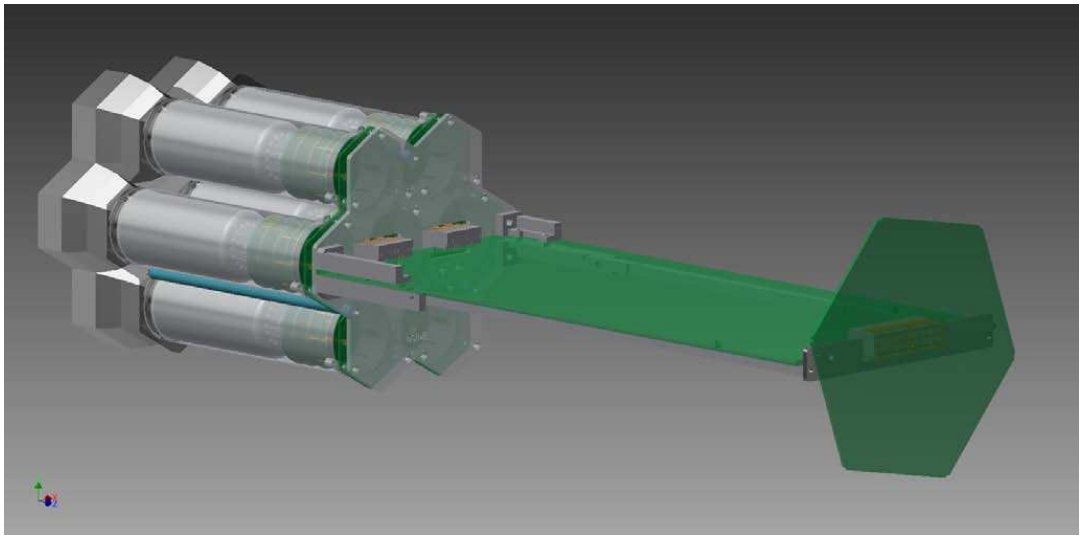

Figure 1. Image of a cluster which is composed of 7 photo-detectors with light guides and a read-out board. The cluster represents the basic unit of the data acquisition system.

on the focal plane which is 28 m away from the center of the mirror. To observe gamma-rays down to 20 GeV, the camera at the LST focal plane must satisfy several requirements:

- high photon detection efficiency
- precise optics geometry
- high speed signal processing
- stable control of devices and precise monitoring
- reduced contamination of Night Sky Background (NSB) and electric noise
- optimized trigger scheme for low energy gamma rays

Based on these requirements, a camera for the first LST is under development. The photons from the mirror are collected by light guides which reduce the dead space in the camera and reject diffuse photons with wide incident angle. The camera of the first LST will be constituted by a set of Photo-Multiplier Tubes (PMTs) developed in collaboration with Hamamatsu Photonics and characterized by high quantum efficiency and low after-pulsing rate. Each PMT has a Cockcroft Walton type High Voltage supply (CW-HV). The HV of each PMT can be adjusted to control the PMT gain. The read-out circuit digitizes the signal from the PMT with a sampling speed of 1 GHz. High accuracy of optics on the focal plane can be achieved based on a structure of the cluster which is composed of 7 PMT modules and the read-out board. A cooling system keeps stable the temperature of these devices during observations. The camera for the first LST will be completed by end of 2015.

Details of the developments of the camera including the focal plane instrument are described in this contribution.

2. THE LST CAMERA

The Focal Plane Instrument (FPI) has a hierarchical structure. Each photo-detector is composed of one PMT, one CW-HV supply and one preamplifier. A group of 7 photo-detectors composes a PMT module. A PMT module and a read-out board compose a cluster. A total of 265 clusters, namely 1855 PMTs, compose the focal plane instrument. The clusters are mounted on a cluster holder which works as a cooling system as well.

Figure 2. A picture of the LG. Three prototype LGs are shown. Basement of the prototype LG is produced by 3D printer. A reflection film is attached on the basement. These prototypes are used for the optimizations of the LG shape together with ray trace simulations.

2.1 Cluster

Figure 1 shows a picture of a cluster. It is assembled in a laboratory and calibrated before to be installed into the cluster holder. The cluster is the basic unit of the data acquisition system including trigger decision. An interface board, so called Slow Control Board (SCB), is placed between the PMT modules and the read-out board so that these devices can be developed independently. The read-out board is connected to a back-plane board which communicates with other clusters, central control, and slow control system of the camera as well as providing DC power. The weight of one cluster is about 1.5 kg.

Light Guide

The diameter of the PMT surface is 40 mm, while the side-to-side diameter of a hexagonal pixel is 50 mm. To reduce the dead space on the focal plane, a hexagonal shape Light Guide (LG) is attached on each PMT. The LG reduces the dead space and guides photons from the mirror to the PMT photo-cathode. Moreover the LG rejects background photons which come from out of the mirror. Reflective cones having inclined parabolic surfaces (Winston cone) are often used for this purpose. The shape of the LG is optimized to guide photons of which incident angle is less than 30 degrees based on a ray-trace simulation.[2] Then, a prototype LGs are produced using a 3D printer so that the machine errors, the production accuracies, and the angler dependence of reflectivity on the incident angle of the photons into the LG surface are included in the optimization. The angular dependence of the quantum efficiency of the PMT surface is also an important factor for this optimization. Figure 2 shows examples of the prototype modules. This procedure is iterated until the optimization is completed. Bézier curve has been also tested.[3] Our latest optimization and measurements show that the Bézier curve with a hexagonal exit window of a side-to-side diameter of 25 mm has higher collection efficiency and background rejection than a normal Bézier cone.

Photo-detector

The PMT R11920-100-20 has been developed with Hamamatsu Photonics and the production for the first LST has been completed. The cathode is a spherical structure with frosted glass that scatters the photons. The spherical structure of the cathode surface increases the probability of the photons of crossing the cathode again. As a result, the quantum efficiency is increased a few %. The peak of the quantum efficiency at 400 nm is 42 % in average and 45 % at maximum, which is significantly improved from that used in previous projects. Folded quantum efficiency with Cherenkov spectrum at about 2 km above sea level is 30 % in average. The PMT is wrapped by a mu-metal sheet, as shown in Figure 3, to reduce the effect of geo-magnetic field. HV on

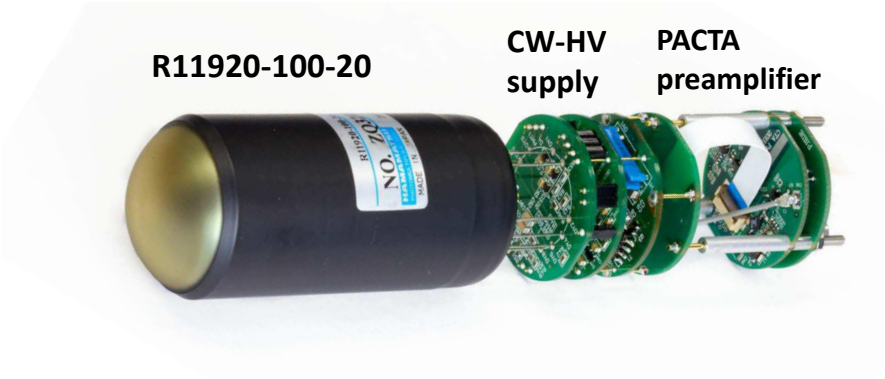

Figure 3. A picture of the PMT Hamamatsu R11920-100-20 adopted in the LST camera. Three boards for CW-HV supply are attached on the PMT. The signal from the PMT anode is transferred to a preamplifier through a co-axial cable.

the first Dynode of this PMT is fixed on 350 V by a Zener diode to reduce signal fluctuation and to increase collection efficiency. Another important parameter is After Pulse (AP). AP is caused by electrons which interact with molecules floating inside the PMT and ionize it. The ionized molecules are moved to the Cathode by the electric field and create additional signal. This signal is called AP and the original signal is called main pulse. AP is defined as the probability of occurrence by a single photoelectron in the main pulse, namely the number of APs divided by the number of main pulses and number of photoelectrons in the main pulses. An AP often contains a few photoelectrons and affects trigger decision. Consequently it may increase threshold energy for the gamma ray. In the PMT R11920-100-20 adopted for the first LST camera, AP is minimized by reducing the contaminations inside the sensor during the production. Chance of occurrence of AP with amplitude higher than 4 photoelectrons has been achieved to be smaller than 0.004 %.

Three PVC boards of CW-HV are soldered to the PMT lines as shown in Figure 3 so that HV of each PMT can be controlled. The NSB during moonless nights is estimated to be around 200 MHz for a single pixel. The anode current is

$$2 \times 10^8[Hz] \times 1.6 \times 10^{-19}[C] \times G = 3.2 \times 10^{-11} \times G[A] \quad (1)$$

where G is the PMT gain. The maximum NSB and G are restricted by the maximum current from CW, which is 100 μA. In addition, a higher HV, means a higher gain, accelerates aging of the PMT. On the other hand, a lower HV makes the pulse width wider. In this case, the effects of NSB in both of the observation and the analysis become significant. Also difference of HV between PMTs makes variation of transit time of the electron in the PMT wider. Therefore, the HV of the all PMTs is designed to be 1000 $\pm$ 100 V. In this configuration, the pulse width from PMT is around 2.9 ns FWHM. The PMT gain, however, cannot be adjusted to be the same for all PMTs in this HV range. Differences of the gain among PMTs are adjusted in the preamplifier boards. The signal from the PMT is transferred to the preamplifier board through a co-axial cable with an impedance of 50 Ω. The signal goes to a divider circuit which adjusts the PMT gain. A percentage of 100, 50 or 30 of the signal goes through the divider circuit and the remaining signal is discarded into the ground line. Finally the gains of the all photo-detectors are adjusted to be 40000. Then the signal is multiplied by a preamplifier ASIC which is called PACTA.[4] PACTA is trans-impedance amplifier and has two gain channels. The high and the low gain of the preamplifier are $\times$24 and $\times$1.6 respectively. Output signals from both of high and low gain channels are differential. Therefore 4 signal lines are connected to later circuits.

The PMT, CW and preamplifier boards are contained in an aluminum pipe of 0.3 mm in thickness. Ground lines of all of the devices in the pipe are tightly connected to the pipe to prevent picking up electrical noises. The pipe also shields the devices electrically. The devices are thermally connected to the cooling system through the pipe.

Slow Control Board

Signals from the PMT module are sent to a read-out board so called Dragon Board (DB) (Figure 4). An interface board, so called Slow Control Board (SCB) are located between the PMT modules and the DB. The

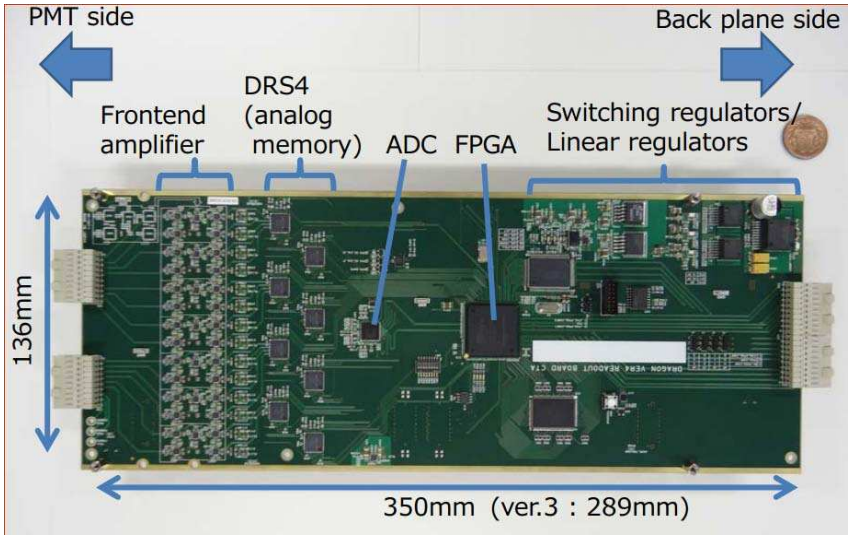

Figure 4. The read-out board for the first LST, so called Dragon Board. The signals from the PMT module are sampled by eight DRS4 chips with 1 GHz sampling speed. When a trigger signal is provided, an ADC digitizes the signal in DRS4.

SCB provides DC power to the PMT modules, monitors HV and anode current, operates CW, reads temperature sensors, and passes signals from the preamplifier board to the DB. The PMT module and the SCB are fixed on a 3 mm thickness aluminum plate. As shown in Figure 1, three aluminum poles are also fixed on this plate. A plastic plate is mounted on these poles and 7 LGs are fixed on this plastic plate. Geometries of the 7 LGs as well as the 7 photo-detectors on the focal plane are determined by this plastic plate. Therefore the aluminum plate, three aluminum poles, and the plastic plate are designed to be fixed precisely. Tolerance of the LG position is 0.5 mm. The photo-detector has a spring mechanics between the CW and the preamplifier board which presses the plastic plate towards the LG to ensure optical contact with them.

Read-Out Board

Each photo-detector provides 4 lines of signals from two gain channels with differential output. Therefore 28 signal lines are connected to DB and go through the main amplifiers. The signals from the high gain channels are sent to trigger circuit and to the high gain channels of the read-out circuit, whereas the low gain signals are sent to low gain channels. The bandwidths of the main amplifiers of high and low gain channels are 300 and 190 MHz respectively. These signals in the high and low gain channels are sent to the Domino Ring Sampler ver.4 (DRS4) ASICs.[5] In the current configuration of the read-out system for the first LST, the signal is continually digitized with 1 GHz sampling and 4096 sampling depth namely 4 μs. The signals recorded in the capacitor array are later digitized by ADCs when a trigger signal is provided. The DB includes eight DRS4 chips, the ADCs, a DAC to control the DRS4, an FPGA, a SRAM, a Gigabit Ethernet transceiver as well as a mezzanine card for the trigger. Total power consumption of one DB is about 17 W during operation.

The NSB can reach up to several 100 MHz in some region of the Galactic plane. To keep the energy threshold as low as possible, the trigger system utilizes the fact that the duration of Cherenkov light from an air-shower is a few nanoseconds. Multi-level trigger schemes select the Cherenkov signals from random triggers caused by the NSB. In a first level, individual telescopes produce a trigger signal out of a small region of pixels in the camera. Combining camera triggers from several telescopes, the final event trigger is formed. The details of the trigger system can be found in.[6]

2.2 Cluster Holder and Cooling System

A total of 265 clusters are mounted on the cluster holder (Figure 5). The cluster is inserted from front side. The LGs are, however, mounted on the front side of the cluster. Therefore the cluster cannot be pushed into the

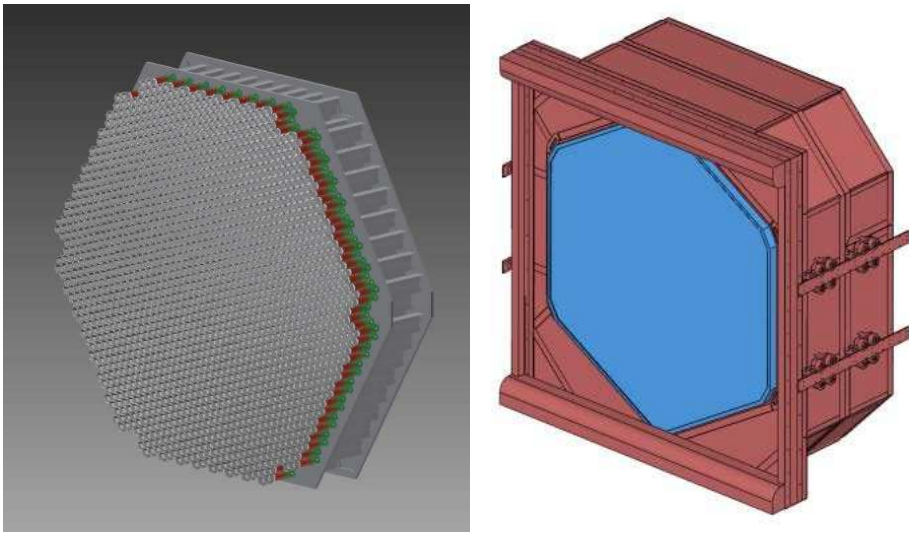

Figure 5. A schematic view of the focal plane instrument and the camera frame. 265 clusters, i.e. 1855 PMTs, are mounted on the cluster holder which has a cooling system. The cluster holder is contained in the camera frame and shielded from the outside environment.

cluster holder. Instead of that the cluster is fixed from backside of the cluster holder. The cluster is connected to the back-plane board and fixed by two screws on the back plane board.

The cluster holder has another important role which is the cooling of the clusters. The amount of power consumption of the camera is more than 6 kW during observation. The heat increases failure rate of the electric devices and may course troubles on the data processing. Therefore, it is important to dissipate the heat and to stabilize temperature in the camera. A water-cooling-heat exchanger is located in the cluster holder and air is circulated by several fans. The coolant water transfers the heat to a chiller which is mounted on the basement of the telescope. Also the coolant water is circulated in the front plate of the cluster holder which works as a cooling plate as well. PMT modules and SCBs are thermodynamically connected to this cooling plate.

2.3 Camera Frame

The cluster holder is mounted on a camera frame after installing 265 clusters. The cluster holder slides into the camera frame from front side. The position of the cluster holder is adjustable after the mounting. The FPI devices have to be designed to work a few tens of years without repair or maintenance. Therefore it is important to shield the camera frame and to isolate the devices in the camera from outside environments. For this purpose the aperture of the camera is covered by a UV transparent glass. A white screen is mounted on the front of the window. It is used to measure star tracks for calibrations and tests. In addition, a shutter is mounted in front of the screen to protect the window. The shutter is obviously opened during observation. Both of the screen and the shutter are controlled from remote.

3. SUMMARY

A camera for the LST of the CTA observatories is being developed. Aperture of the camera is 2.3 m in diameter. Signals from the 1855 pixels of PMTs with 42 % quantum efficiency are digitized with 1 GHz sampling and 300 MHz band width. The pixel size is 50 mm which corresponds to 0.1 degree.

PMTs for the first LST camera has been delivered already and electronics boards are in the mass production. This camera will be completed by end of 2015, then the final test and calibration will be performed before assembly on the first LST in 2016.

3.1 Acknowledgments

We gratefully acknowledge financial support from the following agencies and organizations:

Ministerio de Ciencia, Tecnología e Innovación Productiva (MinCyT), Comisión Nacional de Energía Atómica (CNEA), Consejo Nacional de Investigaciones Científicas y Técnicas (CONICET), Argentina; State Committee of Science of Armenia, Armenia; Conselho Nacional de Desenvolvimento Científico e Tecnológico (CNPq), Fundação de Amparo à Pesquisa do Estado do Rio de Janeiro (FAPERJ), Fundação de Amparo à Pesquisa do Estado de São Paulo (FAPESP), Brasil; Croatian Science Foundation, Croatia; Ministry of Education, Youth and Sports, MEYS LE13012, 7AMB12AR013, Czech Republic; Ministry of Higher Education and Research, CNRS-INSU and CNRS-IN2P3, CEA-Irfu, ANR, Regional Council Ile de France, Labex ENIGMASS, OSUG2020 and OCEVU, France; Max Planck Society, BMBF, DESY, Helmholtz Association, Germany; Department of Atomic Energy, Department of Science and Technology, India; Istituto Nazionale di Astrofisica (INAF), MIUR, Italy; ICRR, University of Tokyo, JSPS, Japan; Netherlands Research School for Astronomy (NOVA), Netherlands Organization for Scientific Research (NWO), Netherlands; The Bergen Research Foundation, Norway; Ministry of Science and Higher Education, the National Centre for Research and Development and the National Science Centre, Poland; MINECO support through the National R+D+I, CDTI funding plans and the CPAN and MultiDark Consolider-Ingenio 2010 programme, Spain; Swedish Research Council, Royal Swedish Academy of Sciences, Sweden; Swiss National Science Foundation (SNSF), Ernest Boninchi Foundation, Switzerland; Durham University, Leverhulme Trust, Liverpool University, University of Leicester, University of Oxford, Royal Society, Science and Technologies Facilities Council, UK; U.S. National Science Foundation, U.S. Department of Energy, Argonne National Laboratory, Barnard College, University of California, University of Chicago, Columbia University, Georgia Institute of Technology, Institute for Nuclear and Particle Astrophysics (INPAC-MRPI program), Iowa State University, Washington University McDonnell Center for the Space Sciences, USA.

The research leading to these results has received funding from the European Union's Seventh Framework Programme (FP7/2007-2013) under grant agreement n ° 262053.

REFERENCES

[1] B.S.Acharya et al. *Astropaticle Physics* **43** (2011).
[2] A. Okumura et al. *Proc. 32nd Int. Cosmic Ray Conf. (arXib:1110.4448)* **9**, 210–213 (2011).
[3] Okumura, A. *Astroparticle Physics* **38**, 18–24 (2012).
[4] A Sanuy et al. *JINST* **7**, C01100 (2012).
[5] S. Ritt, R. Dinapoli, U. H. *NIMA* **623**, 486–488 (2010).
[6] L.A. Tejedor et al. *IEEE Transactions On Nuclear Science* **60**, 2367–2375 (2013).